Magnetism and phase transitions of iron under pressure

Zhao-Yi Zeng[1,2]**, Cui-E Hu**[1,2]**, Xiang-Rong Chen**[1,3,4]**,**
Ling-Cang Cai[2] **and Fu-Qian Jing**[1,2]

[1] School of Physical Science and Technology, Sichuan University, Chengdu 610064,
People's Republic of China
[2] Laboratory for Shock Wave and Detonation Physics Research, Institute of Fluid Physics,
Chinese Academy of Engineering Physics, Mianyang 621900, People's Republic of China
[3] International Centre for Materials Physics, Chinese Academy of Sciences, Shenyang 110016,
People's Republic of China

E-mail: xrchen@126.com

Abstract
The spin-polarized generalized gradient approximation within the plane-wave pseudopotential
density functional theory is employed to investigate the magnetism and phase transition of iron
under pressure. It is found that iron has a ferromagnetic body-centered-cubic (bcc) ground state,
while at high pressure (such as at the Earth's lower mantle and core pressure), the most stable
phase is the nonmagnetic hexagonal-close-packed (hcp) phase. For the face-centered-cubic
(fcc) iron, we find that there is an intermediate-spin state (IS) during the transformation from
the high-spin state (HS) to the low-spin (LS) state under pressure. The transition pressures of
the HS → IS and the IS → LS are about 15 GPa and 50 GPa, respectively. The magnetism can
affect the properties of iron up to 72.9 GPa. From the enthalpy difference between every two
phases, we find the phase transition pressures of FM-bcc → FM-hcp, FM-bcc → NM-hcp and
NM-bcc → NM-hcp are 14.4 GPa, 29.5 GPa and 42.7 GPa, respectively.

1. Introduction

Iron is a material of vital importance to the Earth sciences
and condensed matter physics. The Earth's core is iron
slightly alloyed by Ni and some light elements [1], and the
minor fraction has a small effect on the core's properties.
Thus, to investigate the fundamental properties of the Earth's
core, it is essential to know the behavior of iron. The first
question to resolve is: what is the most stable phase of iron
under high pressure? The phase of iron in a wide pressure
range is of considerable interest for modern technology
and geophysics. The phase diagram of Fe is rather well
described within fluctuation spin theory, showing the strong
magnetovolume coupling. At ambient conditions, the body-
centered-cubic (bcc) phase Fe is stabilized by the presence of
ferromagnetic (FM) moments [2]. Hydrostatic compression
experiments at room temperature showed a transition to the
hexagonal-close-packed (hcp) phase at 13 GPa, with the
reverse transformation taking place at 8 GPa [3]. This
hysteresis declines with increasing temperature, and disappears
at the triple point (about 800 K and 10.5 GPa), and then the
face-centered-cubic (fcc) phase appears [4]. Shock-induced
bcc → hcp transformation occurs at pressures 16.5 GPa [5] and
14.5 GPa [6]. The most often proposed crystalline structure
under high pressure is the nonmagnetic (NM) hcp phase,
although this has been challenged recently at the Earth's core
pressure, with a magnetic body-centered-tetragonal (bct) phase
being suggested [7]. But it is well known that the hcp Fe is
lower in energy than the fcc Fe in the pressure range of 0–400
GPa [8].

It is an intriguing problem that the spontaneous
magnetization occurs in Fe, because the magnetic phenomena
are of extensive applications in technology. Meanwhile,
the fundamental theory is incomplete [9]. Basic issues
surrounding the role of magnetism in the structural stability
remain poorly understood. The surprising discovery of the
electronic high-spin (HS) to low-spin (LS) transition (spin-
pairing transition) of iron in the lower mantle phases challenges
the classical view, and shows that the Earth's interior core is

[4] Author to whom any correspondence should be addressed.

more complex [10]. Moreover, the magnetic phase transitions of fcc iron is an unsolved problem. It is argued whether there is a metastable ferromagnetic intermediate-spin (IS) state during the transformation from a ferromagnetic HS state to the nonmagnetic LS state under pressure. Jones *et al* [11] reported the first investigation of the topology for atypical spin-polarized charge density in bcc and fcc iron. From the presence of distinct spin topologies, they showed an obvious magnetism change in the fcc iron (HS to LS and LS to paramagnetic). The applied pressure results in a decrease in magnetic moment, which makes the question of magnetic stability in iron generally interesting. Although the earlier diamond anvil cell experimental study [12] suggested that hcp iron is either paramagnetic or weakly ferromagnetic up to 17 GPa at 300 K, later other experiments [13] showed the absence of magnetism in the hcp Fe. More recently, Mössbauer experiments [14] showed an anomalous peak up to 40 GPa. On the other hand, the computations based on density functional theory (DFT) found a ferromagnetic ground state stable up to 50 GPa [15] and 60 GPa [16].

In this work, we will focus on the structures, magnetism and phase transition of iron under high pressure by using the spin-polarized *ab initio* calculations. The results obtained are satisfactory. In section 2, we give a brief description of the theoretical computational methods. The results of the equation of state, magnetism and the phase transitions of iron are presented and analyzed in section 3. Conclusions are drawn in the last section.

2. Computational details

The spin-polarized *ab initio* methods can account for the thermodynamic stability and the decrease of the magnetic moment of iron with increasing pressure [17]. More recently, these computational total energy techniques have been extended to explore the structure and dynamics of liquid iron [18], the effect of magnetism on surface alloys [19] and magnetically induced buckling [20]. We here employ the spin-polarized*ab initio* calculations to investigate the structures, magnetism and phase transition of Fe under pressure. It is known that the LDA (or LSDA) description is not valid for iron and iron-rich transition metal alloys, and it always leads to the fcc or hcp ground state for iron [21]. The generalized gradient approximation (GGA) [22] has also been applied to the structural, elastic, magnetic and vibrational studies of iron [15, 16, 23–27]. In this work, we adopt the Perdew–Wang (PW) exchange–correlation functional [28], which is a suitable tool for 3d elements [23].

Although the non-standard DFT method LDA (or GGA) plus on-site Coulomb interaction approaches U is successful in the description of the strongly correlated systems, its correct parameterization remains problematic, as the determination of U is empirical, method-dependent and with large error bars (around 1 eV) [29]. In the case of Fe, the theoretically determined value of U (5–6 eV [30], 2.1 eV [31], 2.0 eV [29, 32], 1.9 eV [33] and 1 eV [29]) is uncertain. While Tréglia *et al* [34] provide a value for U around 1 eV from the experiment. Therefore this method is not

convincing and reliable. We still use here the standard DFT method, as its validity is testified to in many previous calculations [15, 16, 23–27].

The spin-polarized *ab initio* electronic structure calculations are performed using the plane-wave pseudopotential density functional theory. For nonmagnetic materials, the success of the pseudopotential method is already well established. For magnetic materials, there are only a few previous pseudopotential studies dealing with magnetic pure iron [26]. At earlier times, one can obtain reasonable but not fully satisfactory results for bcc Fe by the pseudopotential method [35]. Later, it has been shown that most of the deficiencies of the early work can be overcome by employing more powerful computational resources [36]. Further work addressed the accurate description of ferromagnetic iron by pseudopotentials together with a plane-wave basis [37] or a linear augmented plane-wave (LAPW) basis [38].
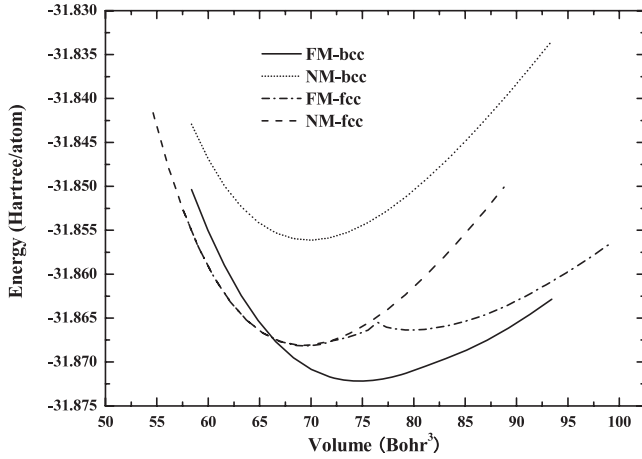
In our calculations, the electronic wavefunctions were expanded in a plane-wave basis set with energy cutoff 500.00 eV. The ultrasoft pseudopotentials introduced by Vanderbilt [39] were employed for all the ion–electron interactions. Pseudo-atomic calculations were performed for Fe $3d^6 4s^2$. As for the Brillouin-zone Monkhorst–Pack meshes, convergence tests gave the k-points separation of 0.042 Å^{-1} (for bcc Fe), 0.043 Å^{-1} (for fcc Fe) and 0.039 Å^{-1} (for hcp Fe). The self-consistent iterations (SCF) were continued until the total energy difference between two consecutive iterations was less than 10^{-6} eV/atom. All the calculations are implemented through the Cambridge Serial Total Energy Package (CASTEP) scheme [40, 41].
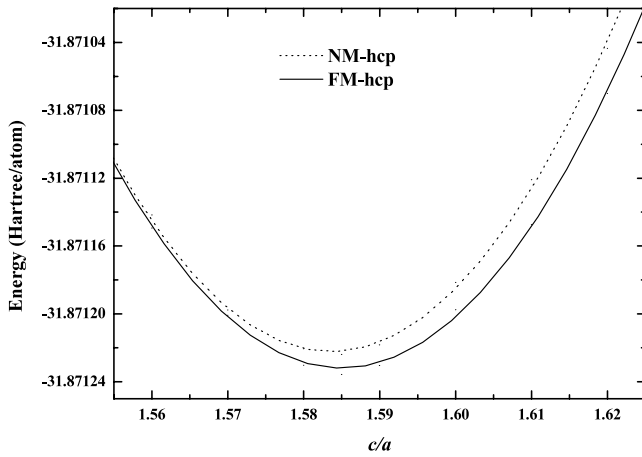
3. Results and discussion

3.1. Equations of state of iron

For both bcc and fcc Fe, we take a series of lattice constants a to obtain the total energy E and the corresponding primitive cell volume V. The results are illustrated in figure 1. The equilibrium volume of the FM state is 75.47 bohr^3. We find an FM-bcc ground state for Fe. This can be understood from the fact that the calculated NM-bcc Fe has no direct physical meaning and cannot be compared with the paramagnetic phase observed in experiments. From the paramagnetic neutron-scattering experiments on the bcc Fe [42], it is known that there is still a substantial magnetic moment in the paramagnetic phase above the Courier temperature.

It is obvious that the E–V curves of the NM- and FM-fcc Fe are nearly the same when the volumes are lower than 70 bohr^3. Meanwhile, there are two minimal energy points on the FM-fcc E–V curve: one is at 69.69 bohr^3 and the other is at 80.53 bohr^3. This double-minimum structure was not obtained by Antropov *et al* [43] by using the linear muffin-tin orbital (LMTO) method. Unfortunately, the result strongly depends on the set of basis functions and the FM state becomes unfavorable if their basis set is expanded. Actually, under compression, the fcc iron transforms from the ferromagnetic high-spin (HS) state to the nonmagnetic state. The latest reports from Jones *et al* [11] showed the critical volume between HS and LS phases is

Figure 1. Energies as functions of primitive cell volume of the bcc and the fcc Fe.

Figure 2. The lowest energy $E_{\min}$ versus c/a for the NM- and FM-hcp Fe.

Table 1. The equilibrium cell volume V_0 (bohr^3), zero pressure bulk modulus B_0 (GPa) and its pressure derivative B'.

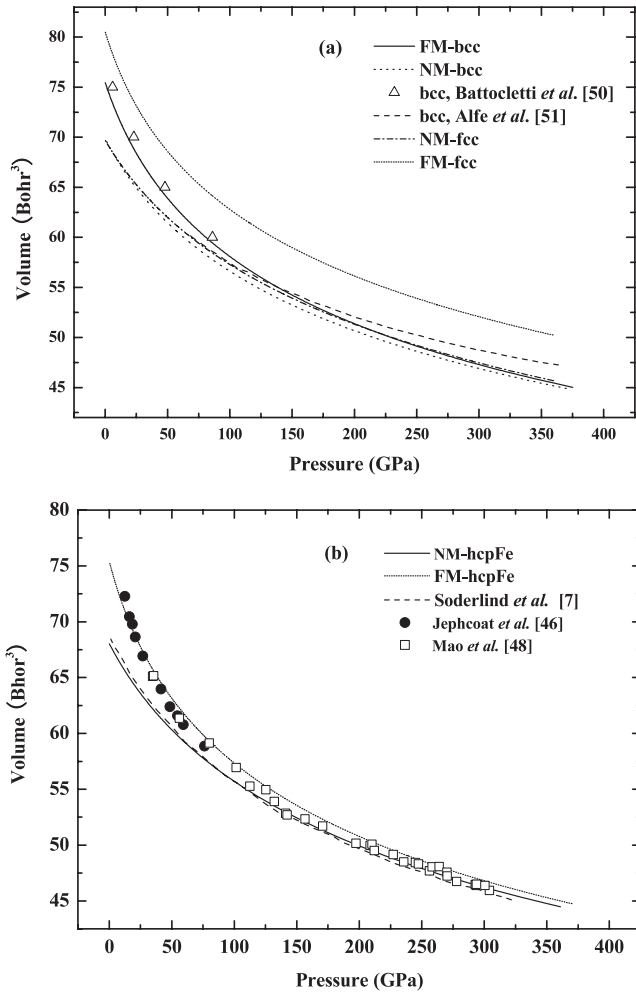|			V_0	B_0	B'
bcc Fe	Present-GGA	NM	69.85	288	4.76
		FM	75.47	199	4.95
	LAPW-GGA [24]	FM	76.84	189	4.9
	LAPW-LSDA [24]	FM	70.73	245	4.6
	LMTO-GGA [25]	FM	75.36	178	4.7
	LAPW-GGA [27]	FM	78.15	185	
	Exp [45]	FM	79.72	173	
	Exp [46]	FM	79.51	172	5.0
fcc Fe	Present-GGA	NM	69.69	329	4.43
		FM	80.53	195	5.83
	LAPW-GGA [23]	NM	69.79	293	
		FM	81.76	171	
	LAPW-GGA [26]	NM	69.58	283	4.8
		FM	81.05	163	4.1
	Exp [47]	NM	76.24		
		FM	81.70		
hcp Fe	Present-GGA	NM	68.03	310	4.75
		FM	75.38	241	6.55
	LAPW-GGA [15]	NM	69.0	292	4.4
		FM	71.2	209	5.2
	TB-GGA [16]	NM	68.8	297	4.6
		FM	70.4	213	6.1
	LAPW-GGA [27]	NM	68.94	263	
	Exp [48]	FM	75.4	165	5.3
	Exp [49]	FM	75.4	164	5.35

the pressure–volume relationship expanded to fourth order in strain is

$$P = 3B_0 f_E (1 + f_E)^{5/2} (1 + \tfrac{3}{2}(B' - 4) f_E$$
$$+ \tfrac{3}{2}(B_0 B'' + (B' - 4)(B' - 3) + \tfrac{35}{9}) f_E^2), \qquad (1)$$

where f_E is written as

$$f_E = [(V_0/V)^{2/3} - 1]/2. \qquad (2)$$

The results are listed in table 1, together with the available experimental data [45–49] and other theoretical results [15, 16, 23–27]. Recently, Stojić and Binggeli [29] reported the FM-bcc structure Fe within LDA + U and GGA + U. Their LDA and LDA + U equilibrium volumes are too small compared to the experimental value in table 1, and their GGA equilibrium volume is much closer to the experimental value. With the inclusion of U^{FLL} (FLL—fully localized limit), the volume increases, but the values are too large, while GGA + U^{AMF} (AMF—around mean field) yields a similar volume to that of GGA. Further increase of U does not alter significantly. It can be seen that the LDA and LDA + U do not seem suitable for Fe and GGA + U has no distinct improvement compared to the standard GGA. The cell volumes of iron as functions of pressure at 0 K are illustrated in figures 3(a) and (b). It is clear in figure 3(a) that the present EOS of the FM-bcc Fe coincides well with the theoretical values by Battocletti *et al* [50], while at higher pressure, there are some small deviations. Our results are a little lower than that from Alfè *et al* [51]. We also illustrated the EOS for the NM- and FM-fcc Fe. In figure 3(b), at lower pressure, the EOS of the FM-hcp Fe coincides well with the experimental values by Jephcoat *et al* [46],

76.3 bohr^3, and the equilibrium volume for the NM phase is 69.3 bohr^3. Our results confirm the results by Jones *et al*. In our work, the HS phase corresponds to $V > 76.36$ bohr^3, while the LS phase occurs for $V \leqslant 76.35$ bohr^3, with the NM phase equilibrating at 69.69 bohr^3.

To determine the equilibrium geometry of the hcp Fe, we followed the following procedures: firstly, for a fixed axial ratio c/a, we took a series of different values of c and a to calculate the total energies E and the corresponding primitive cell volumes V, and then obtained the lowest energy $E_{\min}$ for the given ratio c/a. This procedure was repeated over a wide range of c/a. The $E_{\min}$–c/a curves are shown in figure 2. By fitting a series of $E_{\min}$–c/a data to a second-order polynomial, it is found that the optimized ratio c/a is 1.585 for both NM-hcp Fe and FM-hcp Fe. Meanwhile, we find an FM ground state for the hcp Fe. The equilibrium volume of the FM and NM states is 75.38 bohr^3 and 68.03 bohr^3, respectively.

The zero pressure bulk modulus B_0 and its pressure derivative B' for every structure of Fe are determined by fitting the energy–volume data from *ab initio* calculations to the Birch–Murnaghan equation of state (EOS) [44], in which

Figure 4. Ferromagnetic spin moment versus volume (a) and pressure (b) for the bcc and fcc Fe.

The six electrons (four in t_{2g} orbitals and two in e_g orbitals, corresponding to the high-spin state) result in a magnetic moment of 4 μ_B, μ_B being the Bohr magneton. When atoms are assembled in a crystal, atomic orbital hybridize and form energy bands: the 4s orbital creates a wide band, which remains partially filled; while the 3d↑ and 3d↓ orbitals create narrower bands. Orbital hybridization together with the different bandwidths of the various 3d and 4s bands result in weaker magnetization, equivalent to 2.2 μ_B per atom in bulk iron [9]. The crystal-field splitting energy and the spin-pairing energy can be significantly influenced by pressure. As the applied pressure increases, the electrons are pushed close together and the relative potential energy change between paired and unpaired electrons becomes less important. Under compression, the increase of the splitting energy with respect to the spin-pairing energy ($\Delta_{oct} - \Lambda$) can eventually lead to unpaired 3d electrons of the opposite spin. It means that the unpaired 3d electrons are forced to be paired under pressure.

The magnetic spin moments versus the unit-cell volume and pressure for the FM-bcc and FM-fcc iron are shown in figures 4(a) and (b). Though the magnetism affects the equilibrium volume of the hcp iron, the magnetic moment of the FM-hcp Fe is close to zero. Thus, we did not illustrate the magnetic moment for the FM-hcp Fe here. It is found that the magnetic moments are sensitive to volume (pressure). The moments decrease with decreasing volume (increasing pressure). For the bcc iron, the spontaneous spin polarization is stable over the whole volume range around V_0 ($P = 0$ GPa). The equilibrium value $\mu(V_0)$ 2.14 μ_B is in close accord with many previous calculations (2.13 μ_B by Elsässer *et al* [26], 2.2 μ_B by Hsueh *et al* [17] and 2.21 μ_B by Jones *et al* [11]) and experiment (the total moment $\mu_{exp} = 2.22$ μ_B with dominant spin and 'quenched' orbital contributions of 2.13 μ_B and 0.09 μ_B, respectively [52]). Stojić and Binggeli [29] showed that the moment from standard GGA is in close agreement with the experimental value [23], while the values of GGA+U have large discrepancies. For the fcc iron, the equilibrium magnetic
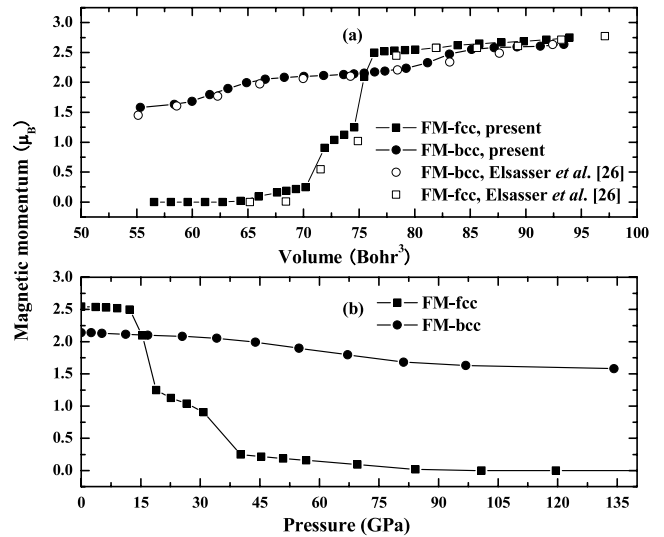
Figure 3. Equations of state for the bcc and fcc Fe (a) and the hcp Fe (b) at 0 K. The open triangles (a), squares (b) and solid circle (b) are the experimental data, while the dashed line (a) is the calculated result.

while at higher pressure, the EOS of the NM-hcp Fe shows good agreement with the experimental results by Mao *et al* [48]. Moreover, our results of the NM-hcp Fe are very close to the theoretical results of Söderlind *et al* [7]. All these results suggest that at lower pressure the stable phase of the hcp Fe is the FM-hcp Fe, while at higher pressure the stable phase is the NM-hcp Fe.

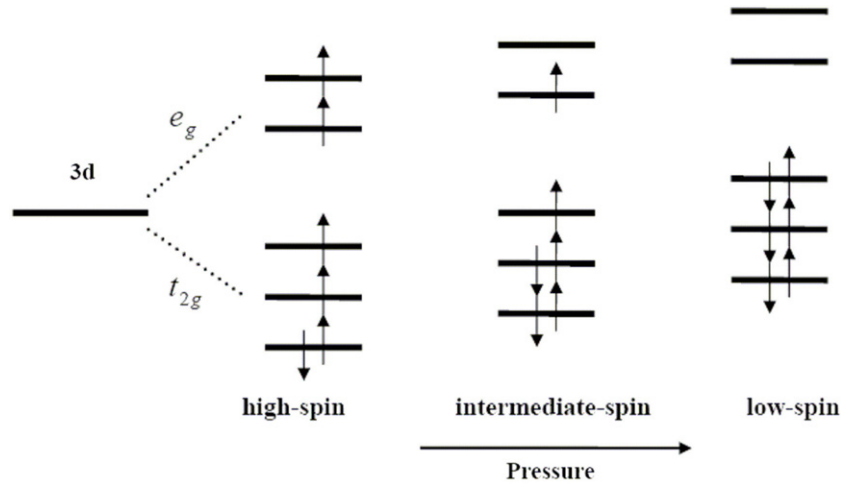## 3.2. Magnetic properties of iron under pressure

The existence of spontaneous magnetization in a metallic system is an intriguing problem because of the extensive technological applications of magnetic phenomena. At the atomic level, ferromagnetism is associated with the partially filled 3d orbital. According to crystal-field theory, the 3d electrons can occupy differently degenerate sets of 3d orbitals, namely the triplet t_{2g} (d_{xy}, d_{xz} and d_{yz}) and doublet e_g (d_z^2 and $d_{x^2-y^2}$) orbitals. The t_{2g} orbitals will be lower in energy than the e_g orbitals. If the splitting energy (Δ_{oct}) between t_{2g} and e_g is smaller than the electron-pairing energy (Λ), the 3d orbital will be occupied according to the simplest Hund's rule.

Figure 5. Construction of 3d orbitals for the fcc Fe in high-spin (left), intermediate-spin (middle) and low-spin (right). The numbers of unpaired electrons are 4, 2 and 0 for the HS, IS and LS states, respectively.

moment is 2.55 μ_B. Our calculations yield the well-known breakdown of the magnetic spin moment for volumes smaller than V_0, from an FM HS state to a metastable FM LS state and finally to the NM state. The HS → LS phase change proceeds through magnetovolume instability. As the volume decreases from the HS phase to the LS phase, the moment has a sudden breakdown. Söderlind *et al* [7] calculated the magnetic moments for all structures of Fe with the FP-LMTO method, but they did not find the HS → LS phase change. Considering the structural and magnetic properties, we can see that the standard GGA within a plane-wave pseudopotential is much more suitable for simulating the properties of Fe.

Meanwhile, during the HS → LS, there are two breakdowns in figure 4. Here, we think there is an intermediate-spin (IS) state between HS and LS states. The construction of HS, IS and LS states for fcc iron are shown in figure 5. When the pressure increases, one electron spin-up in an upper e_g orbital will switch spin and move to the second lowest t_{2g} orbital (IS state, intermediate number of unpaired electrons). When the pressure increase continuously, the other electron in the e_g orbital will also reverse spin and move to the upper t_{2g} orbital (low-spin state, smallest number of unpaired electrons). In other words, iron goes through two pressure-induced partial spin-pairing transitions: upon the first partial spin-pairing transition, the number of unpaired 3d electrons changes from four to two, corresponding to the IS state. After the second partial transition, the number drops to zero, reaching the final LS state. As the volume decreases from the HS state to the IS state, the moment has the first breakdown and the corresponding pressure is about 15 GPa. The second breakdown at about 50 GPa means the transition from IS state to LS state. This point of view is also used to explain the electronic spin state of ferrous iron (Fe^{2+}) in lower mantle perovskite [53]. Pressure-induced spin-paring transitions of ferrous iron have been reported using x-ray emission spectroscopy (46–55 GPa by Lin *et al* [54]), optical absorption (51–60 GPa by Keppler *et al* [55]) and Mössbauer spectroscopy (40–60 GPa by Speziale *et al* [56]).
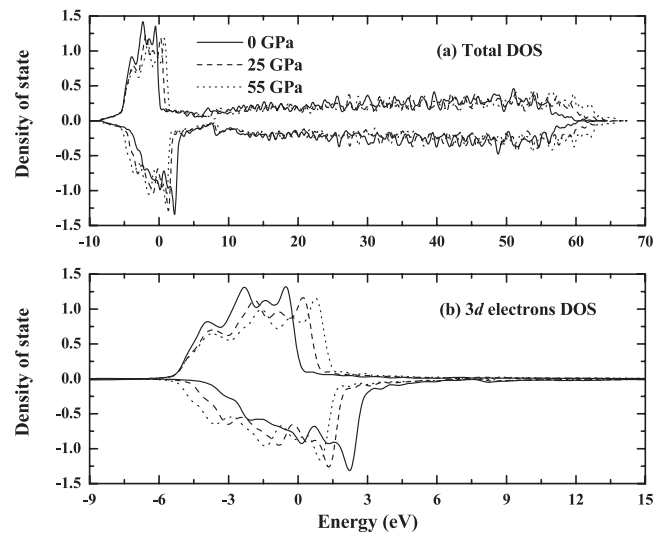
Figure 6. Spin-polarized density of state (DOS) for fcc Fe at different pressures (upper parts of the graphs: $\sigma = \uparrow$; lower parts: $\sigma = \downarrow$): (a) total DOS and (b) partial DOS for 3d electrons.

All the HS → LS transition pressures are around 50 GPa, which can also confirm our result on fcc iron. The successful description of this magnetic structure change is quite difficult in unconstrained spin-polarized calculations [57]. But in our work, it can be easily implemented by a fixed initial spin moment technique.

The results of spin-polarized calculations for the electronic structures of the valence electrons in Fe are presented. Iron with close-packed crystal structures (fcc and hcp) is characterized by very similar properties. Therefore, only the density of state (DOS) for the fcc Fe is discussed as an example. Figure 6(a) shows the total spin-up and spin-down DOS of fcc Fe at different pressures, and (b) shows the partial DOS for 3d electrons. From figure 4, we can see that the structures of FM-fcc Fe at 0, 25 and 55 GPa are HS, IS and LS states, respectively. It is obvious that the spin-up and

spin-down DOS of the LS fcc Fe are symmetrical. So the spin magnetic moments counteract almost entirely. But for HS fcc Fe, the permanent magnetic moment arises from exchange splitting: the $3d^{\uparrow}$ orbital (majority spin) is lower in energy and completely occupied with five electrons, while the $3d^{\downarrow}$ orbital (minority spin) is partially occupied with one electron. When the pressure increases the HS state will be converted to the IS state and then to the LS state. The asymmetry will be suppressed gradually. The main parts of asymmetrical DOS (between -5 and 5 eV) arise almost from the unpaired 3d electrons, as shown in figure 6(b). The DOS for the bcc Fe are also similar to those of the HS fcc Fe, so we did not illustrate them here.

3.3. Phase transitions of iron under pressure

The zero-temperature transition pressure between two phases can be obtained from the usual condition of equal enthalpies H ($H = E + PV$). Then, the phase transition pressures are evaluated by computing the enthalpy differences ΔH at different pressures. Magnetism plays an important role in determining the structure and properties of some 3d transition metal elements. Now we turn our attention to the explicit effect of magnetism on the mechanical stability of the bcc and hcp structures. We find that the magnetization has a direct influence on the mechanical stability of the bcc Fe and the hcp Fe. In general, iron becomes nonmagnetic with increasing pressure. Steinle-Neumann *et al* [16] computed the magnetization energy for various non-collinear ordered spin configurations and predicted that the FM-hcp Fe is stable up to 60 GPa. Here, we obtain the magnetic stability of the bcc Fe and the hcp Fe by calculating the enthalpy differences $H_{FM-bcc} - H_{NM-bcc}$ and $H_{FM-hcp} - H_{NM-hcp}$. The enthalpy differences versus pressure are illustrated in figure 7. Obviously, at low pressure, the FM phase is much more stable than the NM phase, while at high pressure the lower enthalpy makes the NM phase the favorite structural choice over the FM phase. By fitting the ΔH–P data to second-order polynomials, we have the following relations:

$$H_{FM-bcc} - H_{NM-bcc} = -5.05 \times 10^{-7}P^2 + 2.10 \times 10^{-4}P$$
$$- 5.23 \times 10^{-3} \tag{3}$$

$$H_{FM-hcp} - H_{NM-hcp} = -3.32 \times 10^{-7}P^2 + 9.00 \times 10^{-5}P$$
$$- 4.80 \times 10^{-3}. \tag{4}$$

It is found that the phase transitions from the FM phase to the NM phase for the bcc and hcp Fe occur at 26.6 GPa and 72.9 GPa, respectively. Our results show that the magnetism can affect the properties of iron up to 72.9 GPa, which is consistent with the result by Steinle-Neumann *et al* [16].

Generally speaking, the 3d transition metal Fe should behave more like the nonmagnetic 4d element Ru and the 5d element Os. Considering the free energy which includes the band free energy of the itinerant valence d electrons (include the effect of spin fluctuations) and the repulsive contribution, Hasegawa and Pettifor [2] obtained the well-known hcp → bcc → hcp → fcc structural trend across the nonmagnetic 4d and 5d transition metal series. This model is developed to be a bond-order potential and can be used widely and successfully
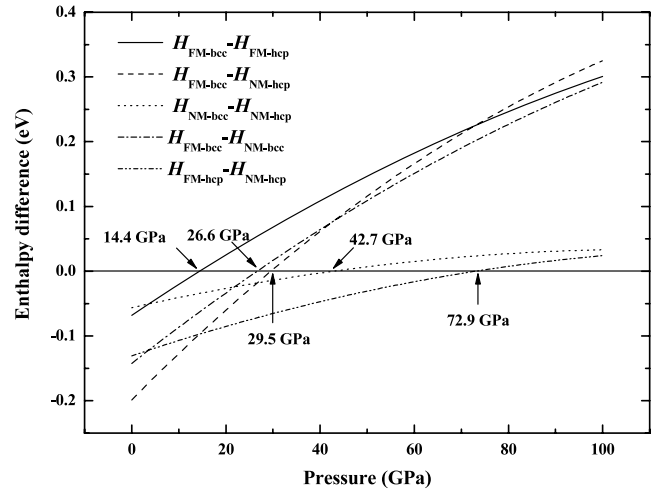

Figure 7. Enthalpy differences as functions of pressure for Fe.

for transition metals [58]. For iron the bcc density of states has a very large peak in the vicinity of the Fermi level, which is not present in the close-packed structures. This allows 3d bcc Fe to satisfy the Stoner criterion $U\rho_0(\varepsilon) > 1$ for the onset of ferromagnetism, whereas the fcc and hcp Fe are unable to do so at their equilibrium volumes [59]. The narrow 3d band and high peak in the density of states at the Fermi level in nonmagnetic iron help to stabilize a large magnetic moment and drive the bcc phase to be more stable than the nonmagnetic hcp phase at low temperatures and pressure. Under pressure, the magnetic energy decreases as the band broadens and the bcc Fe transforms to the hcp phase [58]. Kadau *et al* [4] obtained the transition pressure of about 15 GPa using the Voter–Chen potential. We also investigate the phase transition between the bcc and the hcp phases (shown in figure 7). Similar to above, the relations between the bcc and the hcp are as follows:

$$H_{FM-bcc} - H_{FM-hcp} = -4.44 \times 10^{-7}P^2 + 1.80 \times 10^{-4}P$$
$$- 2.50 \times 10^{-3} \tag{5}$$

$$H_{FM-bcc} - H_{NM-hcp} = -7.76 \times 10^{-7}P^2 + 2.70 \times 10^{-4}P$$
$$- 7.30 \times 10^{-3} \tag{6}$$

$$H_{NM-bcc} - H_{NM-hcp} = -2.71 \times 10^{-7}P^2 + 6.00 \times 10^{-5}P$$
$$- 2.07 \times 10^{-3}. \tag{7}$$

The phase transition from the FM-bcc to the FM-hcp occurs at 14.4 GPa, consistent with the experimental data [3, 5, 6] and theoretical value [16]. Also, the transition pressures from the FM-bcc to the NM-hcp and from the NM-bcc to the NM-hcp are 29.5 GPa and 42.7 GPa, respectively. Ekman *et al* [27] obtained a transition from the FM-bcc to the NM-hcp phase when the applied pressure exceeded 10.3 GPa. But actually the NM-hcp phase in [27] is the FM-hcp phase. Though the magnetic moment is nearly zero, the influence of magnetism does not disappear. It means that 10.3 GPa obtained by Ekman *et al* is the transition pressure from the FM-bcc to the FM-hcp. Comparing all structures of Fe, we find the enthalpy of the NM-hcp phase is the lowest at high pressure, which confirms that the NM-hcp is the most stable structure under high pressure.

4. Conclusions

We have applied the spin-polarized generalized gradient approximation (GGA) within the plane-wave pseudopotential density functional theory (DFT) to investigate the equation of state, magnetism and phase transitions of iron under pressure. It is found that iron has an FM-bcc ground state, while at high pressure (such as at Earth's lower mantle and core pressure), the most stable phase is the NM-hcp phase. The fcc iron transforms from a ferromagnetic HS state to a metastable ferromagnetic LS state and finally to the nonmagnetic state. Moreover, we think that there is an intermediate-spin state (IS) during the transform from the high-spin state (HS) to the low-spin (LS) state. The transition pressures of the HS $\rightarrow$ IS and the IS $\rightarrow$ LS are about 15 GPa and 50 GPa, respectively. The magnetism can affect the properties of iron up to 72.9 GPa. From the enthalpy difference between every two phases, we have found the phase transition pressures of the FM bcc-FM hcp phase transition, the FM bcc-NM hcp phase transition and the NM bcc-NM hcp phase transition are 14.4 GPa, 29.5 GPa and 42.7 GPa, respectively.

Acknowledgments

References

[1] Alfe D, Gillan M J and Price G D 2002 *J. Chem. Phys.* **116** 7127
[2] Hasegawa H and Pettifor D G 1983 *Phys. Rev. Lett.* **50** 130
[3] Wassermann E F, Acet M, Entel P and Pepperhoff W 1999 *Phys. Status Solidi* **82** 2911
[4] Kadau K, Germann T C, Lomdahl P S and Holian B L 2005 *Phys. Rev. B* **72** 064120
[5] Veeser L, Gray G T, Vorthman J, Rodriguez P, Hixson R and Hayes D 2000 *AIP Conf. Proc.* **505** 73
[6] Boettger J C and Wallace D C 1997 *Phys. Rev. B* **55** 2840
[7] Söderlind P, Moriarty J A and Willis J M 1996 *Phys. Rev. B* **53** 14063
[8] Stixrude L, Cohen R E and Singh D J 1994 *Phys. Rev. B* **50** 6442
[9] Tiago M L, Zhou Y, Alemany M M G, Saad Y and Chelikowsky J R 2006 *Phys. Rev. Lett.* **97** 147201
[10] Lin J F, Vankó G, Jacobsen S D, Iota V, Struzhkin V V, Prakapenka V B, Kuznetsov A and Yoo C S 2007 *Science* **317** 1740
[11] Jones T E, Eberhart M E and Clougherty D P 2008 *Phys. Rev. Lett.* **100** 017208
[12] Gilder S and Glen J 1998 *Science* **279** 72
[13] Merkel S, Goncharov A F, Mao H K, Gillet P and Hemley R J 2000 *Science* **288** 1626
[14] Nasu S, Sasaki T, Kawakami T, Tsutsui T and Endo S 2002 *J. Phys.: Condens. Matter* **14** 11167
[15] Steinle-Neumann G and Stixrude L 1999 *Phys. Rev. B* **60** 791
[16] Steinle-Neumann G, Cohen R E and Stixrude L 2004 *J. Phys.: Condens. Matter* **16** S1109
[17] Hsueh H C, Crain J, Guo G Y, Chen H Y, Lee C C, Chang K P and Shih H L 2002 *Phys. Rev. B* **66** 052420
[18] Alfè D, Kresse G and Gillan M J 2000 *Phys. Rev. B* **61** 132
[19] Hong S C, Tim M Y and Freeman A J 1998 *J. Appl. Phys.* **83** 7016
[20] Wuttig M, Gauthier Y and Blugel S 1993 *Phys. Rev. Lett.* **70** 3619
[21] Häglund J 1993 *Phys. Rev. B* **47** 566
[22] Hammer B, Hansen L B and Norskov J K 1999 *Phys. Rev. B* **59** 7413
[23] Herper H C, Hoffmann E and Entel P 1999 *Phys. Rev. B* **60** 3839
[24] Stixrude L, Cohen R E and Singh D J 1994 *Phys. Rev. B* **50** 6442
[25] Sha X and Cohen R E 2006 *Phys. Rev. B* **73** 104303
[26] Elsässer C, Zhu J, Louie S G, Fähnle M and Chan C T 1998 *J. Phys.: Condens. Matter* **10** 5081
[27] Ekman M, Sadigh B, Einarsdotter K and Blaha P 1998 *Phys. Rev. B* **58** 5296
[28] Perdew J P and Wang Y 1992 *Phys. Rev. B* **45** 13244
[29] Stojić N L and Binggeli N L 2008 *J. Magn. Magn. Mater.* **320** 100
[30] Anisimov V I and Gunnarsson O 1991 *Phys. Rev. B* **43** 7570
[31] Cococcioni M and de Gironcoli S 2005 *Phys. Rev. B* **71** 035105
[32] Yang I, Savrasov S Y and Kotliar G 2001 *Phys. Rev. Lett.* **87** 216405
[33] Steiner M M, Albers R C and Sham L J 1992 *Phys. Rev. B* **45** 13272
[34] Tréglia G, Desjonquéres M C, Ducastelle F and Spanjaard D 1981 *J. Phys. C: Solid State Phys.* **14** 4347
[35] Greenside H S and Schlüter M A 1983 *Phys. Rev. B* **27** 3111
[36] Zhu J, Wang X W and Louie S G 1992 *Phys. Rev. B* **45** 8887
[37] Sasaki T, Rappe A M and Louie S G 1995 *Phys. Rev. B* **52** 12760
[38] Cho J H and Scheffler M 1996 *Phys. Rev. B* **53** 10685
[39] Vanderbilt D 1990 *Phys. Rev. B* **41** 7892
[40] Payne M C, Teter M P, Allen D C, Arias T A and Joannopoulos J D 1992 *Rev. Mod. Phys.* **64** 1045
[41] Milman V, Winkler B, White J A, Packard C J, Payne M C, Akhmatskaya E V and Nobes R H 2000 *Int. J. Quantum Chem.* **77** 895
[42] Brown P J, Capellmann H, Déportes J, Givord D and Ziebeck K R A 1982 *J. Magn. Magn. Mater.* **30** 243
[43] Antropov V P, Katnelson M I, Harmon B N, Schilfgaarde M and Kusnezov D 1996 *Phys. Rev. B* **54** 1019
[44] Birch F 1947 *Phys. Rev.* **71** 809
[45] Harrison R, Voter A F and Chen S P 1989 *Atomistic Simulation of Materials* ed V Vitek and D J Srolovitz (New York: Plenum) p 219
[46] Jephcoat A P, Mao H K and Bell P M 1986 *J. Geophys. Res.* **91** 4677
[47] Acet M, Zähres H and Wassermann E F 1994 *Phys. Rev. B* **49** 6012
[48] Mao H K, Wu Y, Chen L, Shu J and Jephcoat A P 1990 *J. Geophys. Res.* **95** 21737
[49] Anderson O L, Dubrovinsky L, Saxena S K and LeBihan T 2001 *Geophys. Res. Lett.* **28** 399
[50] Battocletti M, Ebert H and Akai H 1996 *Phys. Rev. B* **53** 9776
[51] Alfè D, Price G D and Gillan M J 2001 *Phys. Rev. B* **64** 045123
[52] *Landolt–Börnstein New Series Group III* 1987 vol 19a (Berlin: Springer)
[53] Li J, Struzhkin V V, Mao H K, Shu J, Hemley R J, Fei Y, Mysen B, Dera P, Prakapenka V and Shen G 2004 *Proc. Natl Acad. Sci. USA* **101** 14027
[54] Lin J F, Struzhkin V V, Gavriliuk A G and Lyubutin I 2007 *Phys. Rev. B* **75** 177102
[55] Keppler H, Kantor I and Dubrovinsky L S 2007 *Am. Mineral.* **92** 433
[56] Speziale S, Milner A, Lee V E, Clark S M, Pasternak M and Jeanloz R 2005 *Proc. Natl Acad. Sci.* **102** 17918
[57] Moruzzi V L, Marcus P M, Schwarz K and Mohn P 1986 *Phys. Rev. B* **34** 1784
[58] Drautz R and Pettifor D G 2006 *Phys. Rev. B* **74** 174117
[59] Pettifor D G 1972 *Metallurgical Chemistry* ed O Kubaschewski (London: HMSO) p 191